A Bond-Graph Representation of a Two-Gimbal Gyroscope

Robert T. Mc Bride
Raytheon Missile Systems
P.O. Box 11337, Bldg. 805, M/S M-4
Tucson, AZ, 85734-1337, USA
rtmcbride@west.raytheon.com

François E. Cellier
University of Arizona
P.O. Box 210104,
Tucson, AZ, 85721-0104, USA
cellier@ece.arizona.edu

Keywords: bond-graph, gyroscope, Lagrangian, state-variable reduction.

Abstract

The purpose of this paper is to show, by example of a two-gimbal gyroscope, a method for developing a bond-graph representation of a system from the Lagrangian. Often the Lagrangian of a system is readily available from texts or other sources. Although the system equations can be derived directly from the Lagrangian there is still benefit in viewing the system in bond-graph representation. Viewing the power flow through the system gives insight into the inter-relationships of the state variables. This paper will give an example where the possibility of reducing the order of the system is obvious when viewing the system in bond-graph representation yet is not readily apparent when looking at the Lagrangian or the equations derived from the Lagrangian.

INTRODUCTION

The two-gimbal gyroscope, shown in Figure 1, is a system described by three generalized coordinates, which results in a four-state variable system. Classical analysis has shown that under certain conditions, the four-state variable system can be reduced to a three-state variable system [1]. This analysis is immediately apparent from the bond-graph model of the gyroscope.

An alternative bond-graph representation of this system can be found in the paper *Three-axis platform simulation: Bond graph and Lagrangian Approach* by Tiernego and van Dixhoorn [2]. The two representations are distinct due to separate methods of bond-graph derivation.

LAGRANGE METHOD

The system can be simplified by setting the distance *l*, shown in Figure 1, to zero. This will cause the potential energy term in the Lagrangian to disappear.

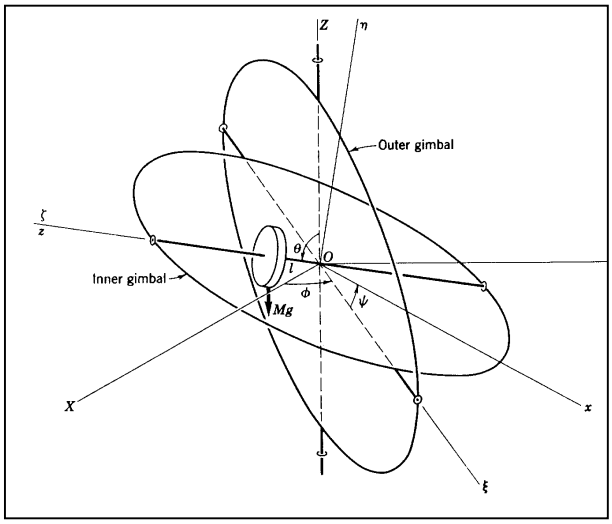

Figure 1. Two-Gimbal Gyroscope

The resulting Lagrangian is then equal to the kinetic energy term only, i.e.:

$$L = T = \frac{1}{2}\left[(A + A')\dot{\theta}^2 + (A + B')\dot{\phi}^2 \sin^2\theta + C(\dot{\phi}\cos\theta + \dot{\psi})^2 + C'\dot{\phi}^2\cos^2\theta + C''\dot{\phi}^2\right] \quad (1)$$

Where θ, ϕ, and ψ, the three Euler angles, are the generalized coordinates of the system. The moment of inertia of the rotor about the symmetry axis ζ is denoted as C, and A is the moment of inertia of the rotor about any transverse axis through the point *O*. The moments of inertia of the inner gimbal about the axes ξ, η, and ζ, are denoted by A', B', and C', respectively. The moment of inertial of the outer gimbal about the inertial axis Z is denoted by C''. The corresponding Lagrange equations are:

$$N_\phi = \frac{d}{dt}\left(\frac{\partial L}{\partial \dot{\phi}}\right) - \frac{\partial L}{\partial \phi}. \quad (2)$$

$$N_\phi = (A+B')\ddot{\phi}\sin^2\theta + 2(A+B')\dot{\phi}\dot{\theta}\sin\theta\cos\theta + C(\ddot{\phi}\cos\theta - \dot{\phi}\dot{\theta}\sin\theta + \ddot{\psi})\cos\theta - C(\dot{\phi}\cos\theta + \dot{\psi})\dot{\theta}\sin\theta + C'\ddot{\phi}\cos^2\theta - 2C'\dot{\phi}\dot{\theta}\sin\theta\cos\theta + C''\ddot{\phi}. \quad (3)$$

$$N_\psi = \frac{d}{dt}\left(\frac{\partial L}{\partial \dot{\psi}}\right) - \frac{\partial L}{\partial \psi} = = C(\ddot{\phi}\cos\theta - \dot{\phi}\dot{\theta} + \ddot{\psi}). \quad (4)$$

$$N_\theta = \frac{d}{dt}\left(\frac{\partial L}{\partial \dot{\theta}}\right) - \frac{\partial L}{\partial \theta} = = (A+A')\ddot{\theta} + C(\dot{\phi}\cos\theta + \dot{\psi})\dot{\phi}\sin\theta - (A+B'-C')\dot{\phi}^2\sin\theta\cos\theta. \quad (5)$$

Where N_ϕ, N_ψ, and N_θ are the generalized torques. The Lagrangian equations are three-, second order-, coupled-differential equations resulting in a sixth-order system. The state variables of this system are $\theta, \dot{\theta}, \phi, \dot{\phi}, \psi,$ and $\dot{\psi}$. However, the state variables ϕ, and ψ do not show up in the above equations. Thus the system can be described entirely by four state-equations. The four state-equations consist of equations 3, 4, 5, and the trivial equation give by equation 6. The resulting system is a fourth-order, non-linear system.

$$\dot{\theta} = \frac{d}{dt}(\theta) \quad (6)$$

BOND-GRAPH DEVELOPMENT

A summary of the method used to derive the bond-graph from the Lagrangian is as follows:

- Note the flow terms in the Lagrangian. These terms come from the kinetic energy portion of the Lagrangian formulation. Assign a one junction for each of the separate flow terms and an appropriate C/I element where necessary.
- Derivate each of the terms of the Lagrangian with respect to time. This transforms the Lagrangian energy terms into power terms. These power terms will be in the form of effort * flow, or more generally, effort * (sum of flows).
- The sum of flows can now be drawn in bond-graph form by placing 0-junctions and connecting the appropriate 1-junctions. The direction of the power arrows will be apparent from the signs on the power terms derived from the previous step.
- All of the terms of the bond-graph are now present but further connections may be necessary to complete the bond-graph. These connections will be apparent by inspecting the terms of the Lagrange equations that are not yet represented by the bond-graph.

An application of these steps is shown using the two-gimbal gyroscope as an example.

Bond-Graph Development of the Two-Gimbal Gyroscope

Naturally, since the only energy storage devices in this system are inertias, the potential energy terms from the Lagrangian in equation 1, all have the from *½*I*flow²*. After writing all five terms of the Lagrangian in this form, it is apparent that the bond-graph will have at least five 1-junctions defined by the following flows:

$$Flow_1 = \dot{\theta}. \quad (7)$$

$$Flow_2 = \dot{\phi}. \quad (8)$$

$$Flow_3 = \dot{\phi}\cos\theta + \dot{\psi}. \quad (9)$$

$$Flow_4 = \dot{\phi}\cos\theta. \quad (10)$$

$$Flow_5 = \dot{\phi}\sin\theta. \quad (11)$$

Derivating each of the terms of the Lagrangian with respect to time gives power. This results in the five power terms:

$$Power_1 = \frac{d}{dt}\left[\frac{1}{2}(A+A')\dot{\theta}^2\right] = (A+A')\dot{\theta}\ddot{\theta}. \quad (12)$$

$$Power_2 = \frac{d}{dt}\left[\frac{1}{2}C''\dot{\phi}^2\right] = C''\dot{\phi}\ddot{\phi}. \quad (13)$$

$$Power_3 = \frac{d}{dt}\left[\frac{1}{2}C(\dot{\phi}\cos\theta + \dot{\psi})^2\right] = = C(\dot{\phi}\cos\theta + \dot{\psi})(\ddot{\phi}\cos\theta - \dot{\phi}\dot{\theta}\sin\theta + \ddot{\psi}). \quad (14)$$

$$Power_4 = \frac{d}{dt}\left[\frac{1}{2}C'\dot{\phi}^2\cos^2\theta\right] =$$
$$= C'\dot{\phi}\ddot{\phi}\cos^2\theta - C'\dot{\phi}^2\dot{\theta}\sin\theta\cos\theta. \quad (15)$$

$$Power_5 = \frac{d}{dt}\left[\frac{1}{2}(A+B')\dot{\phi}^2\sin^2\theta\right] =$$
$$= (A+B')\dot{\phi}\ddot{\phi}\sin^2\theta +$$
$$+ (A+B')\dot{\phi}^2\dot{\theta}\sin\theta\cos\theta. \quad (16)$$

Dividing equations 12 through 16 by their corresponding flows in equations 7 through 11, respectively, produces the five efforts that correspond to the *I* elements on the five 1-junctions. The resulting efforts are:

$$Effort_1 = (A+A')\ddot{\theta}. \quad (17)$$

$$Effort_2 = C''\ddot{\phi}. \quad (18)$$

$$Effort_3 = C\left(\ddot{\phi}\cos\theta - \dot{\phi}\dot{\theta}\sin\theta + \ddot{\psi}\right). \quad (19)$$

$$Effort_4 = C'\ddot{\phi}\cos\theta - C'\dot{\phi}\dot{\theta}\sin\theta. \quad (20)$$

$$Effort_5 = (A+B')\ddot{\phi}\sin\theta + (A+B')\dot{\phi}\dot{\theta}\cos\theta. \quad (21)$$

These five 1-junctions build the basic structure of the bond-graph. Also, it is clear from equation 9 that a 0-junction is needed to sum two flow signals. The basic bond-graph structure is shown in Figure 2. This structure includes the necessary causality strokes to define the above relationships.

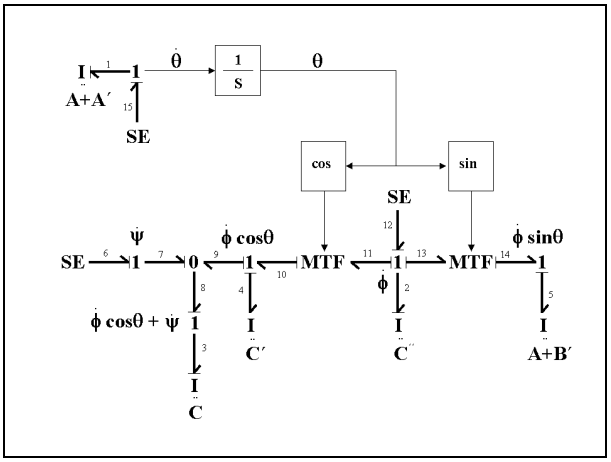

Figure 2. Basic Bond-Graph Structure

Although two of the 1-junctions shown in Figure 2 can be collapsed to a single bond, they have been left so that the flows can be called out specifically. The causalities shown in Figure 2 are the necessary causal marks to produce the equations described above. This system has three integral causal elements, which results in the three degrees of freedom $\dot{\theta}, \dot{\phi}, \text{and } \dot{\psi}$. The trivial equation is obtained by integrating the flow of the $\dot{\theta}$ 1-junction to produce θ. The signal flow of θ has an integrator in its path which increments the order of the system by one, making the bond-graph of Figure 2 a fourth-order system.

The bond-graph of Figure 2 is still incomplete, however. The necessary changes to the bond-graph of Figure 2 can be found by close inspection of equation 5. Re-writing this equation without grouping the terms $(A+B'-C')$ one obtains:

$$N_\theta = (A+A')\ddot{\theta} + C\left(\dot{\phi}\cos\theta + \dot{\psi}\right)\dot{\phi}\sin\theta +$$
$$C'\dot{\phi}^2\sin\theta\cos\theta -$$
$$(A+B')\dot{\phi}^2\sin\theta\cos\theta. \quad (22)$$

Note that the terms

$$C\left(\dot{\phi}\cos\theta + \dot{\psi}\right)\dot{\phi}\sin\theta; \quad (23)$$

$$C'\dot{\phi}^2\sin\theta\cos\theta; \quad (24)$$

and,

$$(A+B')\dot{\phi}^2\sin\theta\cos\theta \quad (25)$$

of equation 22 contain the angular momentums of bonds 3, 4, and 5 of the above bond-graph, respectively. Grouping together the angular momentum terms of bonds 3, 4, and 5 in equations 23 through 25 results in equations 26 through 28.

$$[C\left(\dot{\phi}\cos\theta + \dot{\psi}\right)]\dot{\phi}\sin\theta. \quad (26)$$

$$[C'\dot{\phi}\cos\theta]\dot{\phi}\sin\theta. \quad (27)$$

$$[(A+B')\dot{\phi}\sin\theta]\dot{\phi}\cos\theta \quad (28)$$

One can see that equations 26 through 28 all have the form angular momentum times angular velocity, or in bond-graph terms P*f. These equations can be realized in bond-graph

notation by using gyrators that are modulated by angular momentum [3]. In this case the effort signal is being defined by a flow signal which implies the gyrator causality as shown in Figure 3.

Figure 3. Gyrator Causality

Using the gyrator element of Figure 3 to connect the 1-junctions as described in table 1 completes the bond-graph of Figure 2.

Table 1. Gyrator Connections

1-Junction	1-Junction	Gyrator Modulus
$\dot{\theta}$	$\dot{\phi}\cos\theta$	P_5
$\dot{\theta}$	$\dot{\phi}\sin\theta$	P_3
$\dot{\theta}$	$\dot{\phi}\sin\theta$	P_4

The complete bond-graph is shown in Figure 4. For clarity, the modulated transformer signal paths, shown in Figure 2, have been removed in Figure 4.

An alternative bond-graph for this system is offered by Tiernego and van Dixhoorn [2]. The Tiernego/van Dixhoorn representation is more symmetric than the representation shown here. However, the representation given here is more compact. The modulated gyrators in both representations allow for non-unique bond-graph construction.

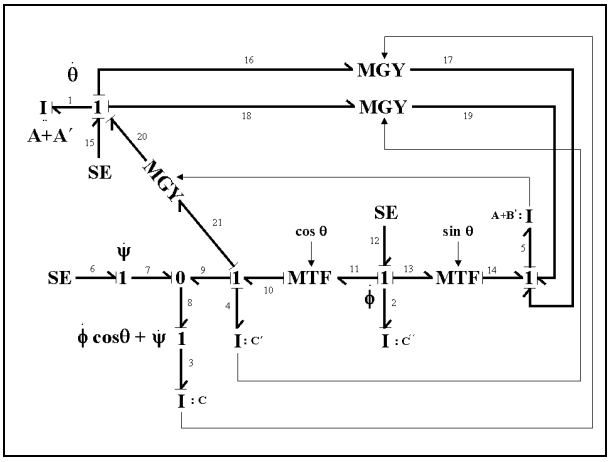

Figure 4. Complete Bond-Graph of the Two-Gimbal Gyroscope

The inputs SE_{15}, SE_{12}, and SE_6 correspond to the respective generalized torques N_θ, N_ϕ, and N_ψ of the above Lagrange equations. In strict bond-graph terminology the equations of the bond-graph of Figure 4 are obtained as follows:

$$P_2 = SE_{12} - e_{11} - e_{13} \tag{29}$$

$$e_{11} = e_{10}\cos\theta \tag{30}$$

$$e_{10} = e_{21} + e_9 + e_4 \tag{31}$$

$$e_{21} = f_{20}P_5 = \frac{P_1P_5}{I_1} \tag{32}$$

$$P_5 = I_5 f_5 = I_5 f_{14} = I_5 f_{13}\sin\theta = \frac{I_5P_2}{I_2}\sin\theta \tag{33}$$

Substituting 33 into 32 yields:

$$e_{21} = \frac{P_1P_2I_5}{I_1I_2}\sin\theta. \tag{34}$$

$$e_9 = e_7 = e_6 = SE_6 \tag{35}$$

$$e_4 = I_4\left[\frac{\dot{P}_2}{I_2}cos\theta - \frac{P_1P_2}{I_1I_2}\sin\theta\right] \tag{36}$$

$$e_{13} = e_{14}\sin\theta \tag{37}$$

$$e_{14} = e_5 - e_{17} - e_{19} \tag{38}$$

$$e_5 = I_5\left[\frac{\dot{P}_2}{I_2}\sin\theta + \frac{P_1P_2}{I_1I_2}\cos\theta\right] \tag{39}$$

$$e_{17} = f_{16}P_3 = \frac{P_1P_3}{I_1} \tag{40}$$

$$e_{19} = f_{18}P_4 = \frac{P_1P_4}{I_1} \tag{41}$$

$$P_4 = \frac{I_4 P_2}{I_2}\cos\theta \tag{42}$$

Substituting 42 into 41 yields:

$$e_{19} = \frac{P_1 P_2 I_4}{I_1 I_2}\cos\theta \tag{43}$$

Substituting the results of equations 30 through 43 into equation 29 and solving for $\dot{P}_2$ yields:

$$\dot{P}_2 = \frac{I_2 I_1 (SE_{12} - SE_6\cos\theta) + P_1 P_3 I_2 \sin\theta}{I_1[I_2 + I_4\cos^2\theta + I_5\sin^2\theta]} + \frac{2P_1 P_2 \sin\theta\cos\theta(I_4 - I_5)}{I_1[I_2 + I_4\cos^2\theta + I_5\sin^2\theta]}. \tag{44}$$

Equation 44 is the first complete equation from the bond-graph of Figure 4.

$$\dot{P}_3 = SE_6 \tag{45}$$

Equation 45 is the second equation from the bond-graph.

$$\dot{P}_1 = SE_{15} + e_{20} - e_{18} - e_{16} \tag{46}$$

$$e_{20} = \left(\frac{P_2}{I_2}\right)^2 I_5 \sin\theta\cos\theta \tag{47}$$

$$e_{18} = \left(\frac{P_2}{I_2}\right)^2 I_4 \sin\theta\cos\theta \tag{48}$$

$$e_{16} = \frac{P_2 P_3}{I_2}\sin\theta \tag{49}$$

Substituting equations 47 through 49 into equation 46, and simplifying, yields:

$$\dot{P}_1 = SE_{15} - \frac{P_2 P_3}{I_2}\sin\theta + \left(\frac{P_2}{I_2}\right)^2 \sin\theta\cos\theta(I_5 - I_4) \tag{50}$$

Equation 50 is the third equation from the bond-graph.

The trivial equation shown in equation 6 has been re-written in equation 51 in pure bond-graph notation.

$$\frac{P_1}{I_1} = \frac{d}{dt}\theta \tag{51}$$

The complete bond-graph equations are given by equations 44, 45, 50 and 51. Equation 44 corresponds to the Lagrange equation given by equation 3. Equation 45 corresponds to the Lagrange equation given by equation 4. Equation 50 corresponds to the Lagrange equation given by equation 5. Note that equation 44 ends up as a function of two effort sources while none of the Lagrange equations end up as a function of two generalized torques. The generalized torque N_ψ can be substituted into equation 3 by observing that the term $C(\ddot{\phi}\cos\theta - \dot{\phi}\dot{\theta}\sin\theta + \ddot{\psi})$ appears in both equations 3 and 4. After this substitution equation 3 becomes

$$\begin{aligned} N_\phi = {} & (A + B')\ddot{\phi}\sin^2\theta + \\ & 2(A + B')\dot{\phi}\dot{\theta}\sin\theta\cos\theta + N_\psi\cos\theta - \\ & C(\dot{\phi}\cos\theta + \dot{\psi})\dot{\theta}\sin\theta + C'\ddot{\phi}\cos^2\theta - \\ & 2C'\dot{\phi}\dot{\theta}\sin\theta\cos\theta + C''\ddot{\phi}. \end{aligned} \tag{52}$$

which is a function of two generalized torques. The bond-graph makes this substitution naturally.

SYSTEM ORDER REDUCTION

Classical analysis has shown that the system order of the two-gimbal gyroscope can be reduced when the inputs N_ϕ, and N_ψ are set to zero [1]. This observation comes naturally to the bond-graph. Assuming that the initial condition on P_3 is zero, and the input SE_6 is zero for all time, then the efforts on bonds 3, 6, 7, 8, and 9 are all zero. They can be removed from the bond-graph, which completely removes the element I_3. The gyrator modulus for the gyrator between bonds 16 and 17 is now zero since the element I_3 has been removed. Thus the power transmitted on bonds 16 and 17 is now zero and they can be removed as well. The resulting simplified bond-graph is shown in Figure 5. Note that this reduced bond-graph is a third-order system. The three state variables from the bond-graph are P_1, P_2, and θ. The resulting bond-graph equations are given by equations 53 and 54.

$$\dot{P}_2 = \frac{I_2 I_1 SE_{12} + 2P_1 P_2 \sin\theta\cos\theta(I_4 - I_5)}{I_1[I_2 + I_4\cos^2\theta + I_5\sin^2\theta]} \qquad (53)$$

$$\dot{P}_1 = SE_{15} + \left(\frac{P_2}{I_2}\right)^2 \sin\theta\cos\theta(I_5 - I_4) \qquad (54)$$

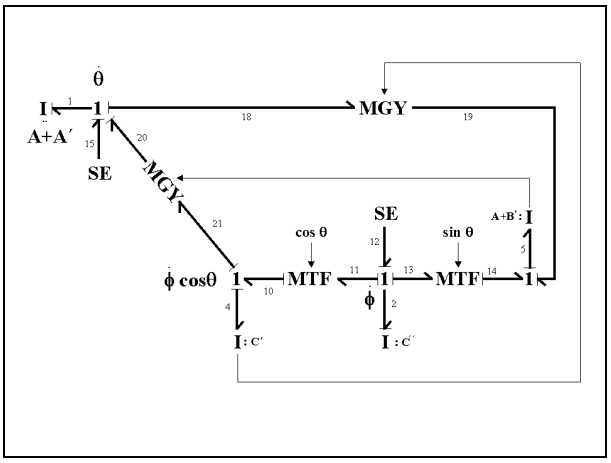

Figure 5. Resulting Bond Graph for $SE_6 = 0.$

For $P_3 = 0$ and $SE_6 = 0$ equations 53 and 54 are identical to equations 44 and 50 respectively. For non-zero initial conditions on P_3 the bond-graph needs to be left in its complete form as show in Figure 4. This allows the equation $\dot{P}_3 = SE_6$ to produce $P_3 = P_{3_0}$ where P_{3_0} is the initial condition on P_3.

DYMOLA SIMULATION RESULTS

DYMOLA [4] was used to simulate both the bond-graph equations, given by equations 44, 45, 50, and 51, and the Lagrange equations given by equations 3, 4, 5, and 6.

The mass values were arbitrarily chosen as $A = 2$, $A' = 1.4$, $B' = 1.2$, $C = 4$, $C' = 2.6$, and $C'' = 2.2$ The generalized torque inputs were modeled as shown in Figure 6. Time plots for the four state variables θ, $\dot{\theta}$, $\dot{\phi}$, and $\dot{\psi}$ are shown in Figures 7 through 9. The error between the two systems is shown in Figures 10 through 14. The variables $\dot{\theta}$, $\dot{\phi}$, and $\dot{\psi}$ are obtained from the bond-graph variables through the transformation equations given by equations 55 through 57, respectively.

The bond-graph simulation results are identical to the Lagrange simulation results. This is no surprise since the bond-graph was obtained directly from the Lagrange equations.

$$\dot{\theta} = \frac{P_1}{I_1} = \frac{P_1}{A + A'} \qquad (55)$$

$$\dot{\phi} = \frac{P_2}{I_2} = \frac{P_2}{C''} \qquad (56)$$

$$\dot{\psi} = \frac{P_3}{I_3} - \frac{P_2}{I_2}\cos\theta = \\ = \frac{P_3}{C} - \frac{P_2}{C''}\cos\theta. \qquad (57)$$

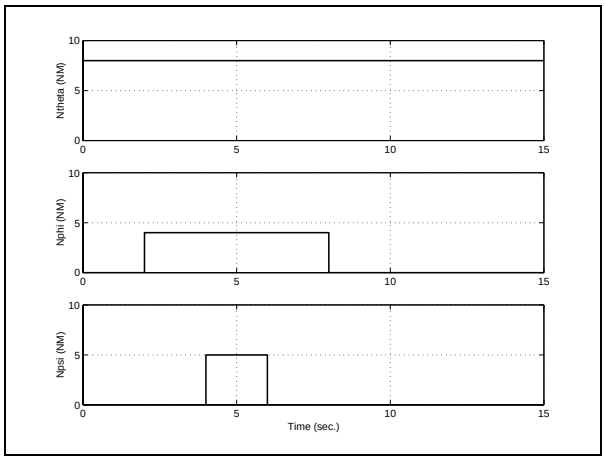

Figure 6. Simulation Input Profiles

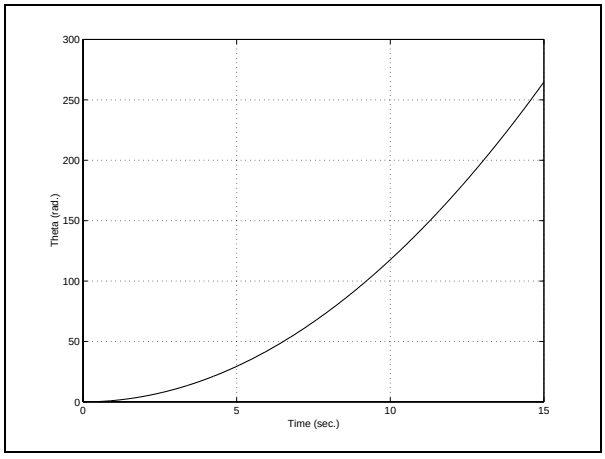

Figure 7. θ Simulation Result

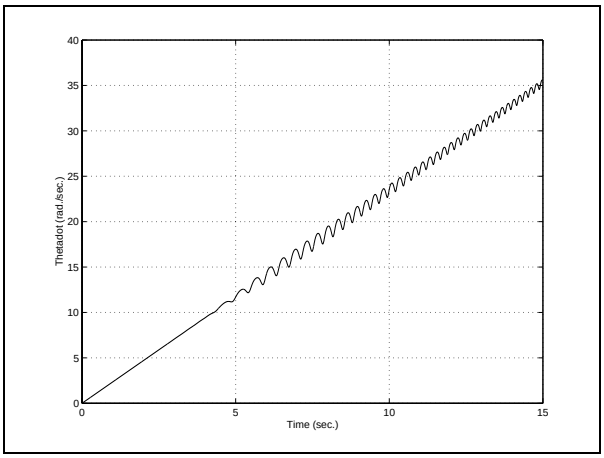

Figure 8. $\dot{\theta}$ Simulation Result

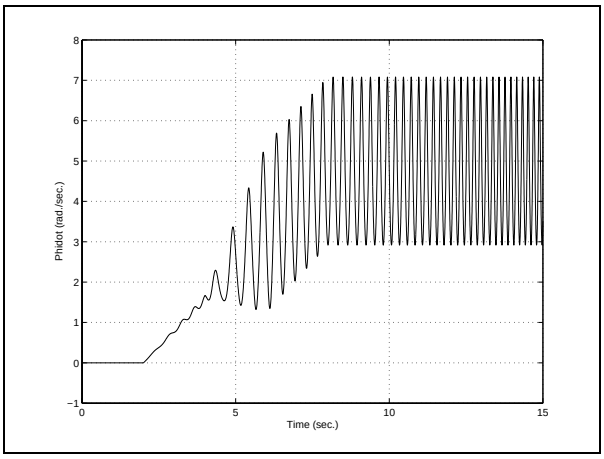

Figure 9. $\dot{\phi}$ Simulation Result

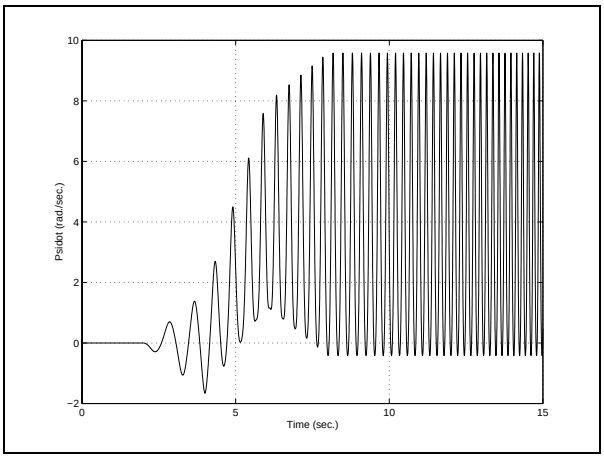

Figure 10. $\dot{\psi}$ Simulation Result

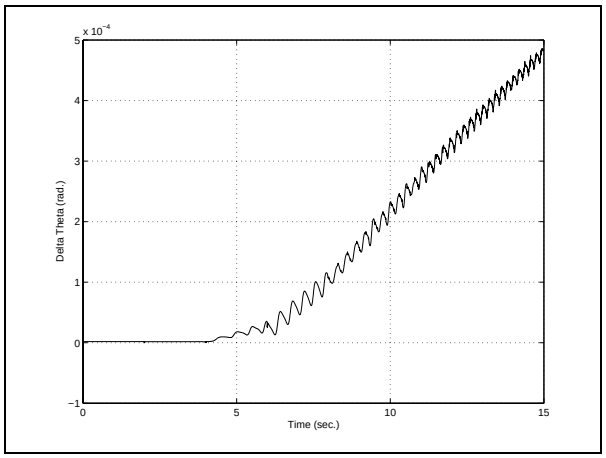

Figure 11. θ Relative Error

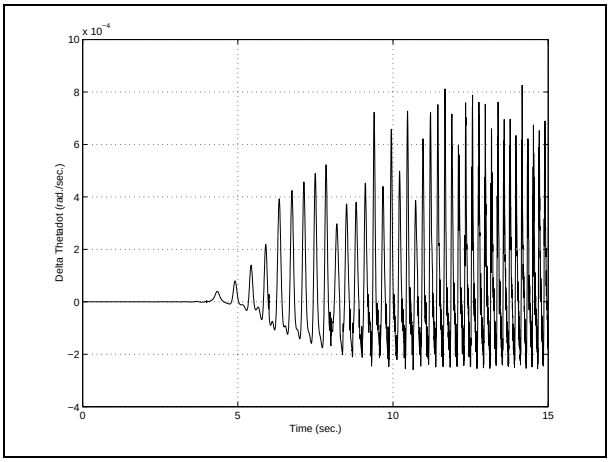

Figure 12. $\dot{\theta}$ Relative Error

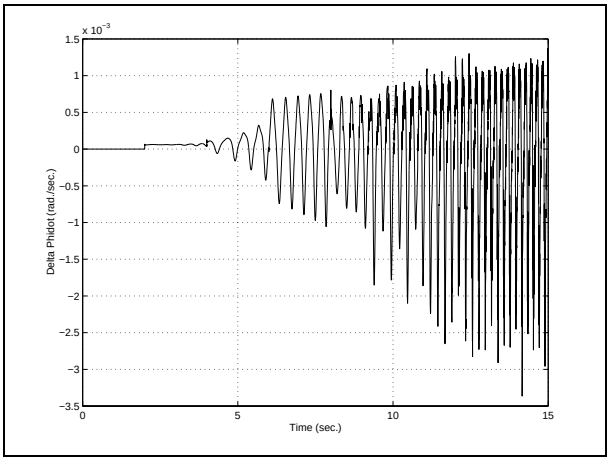

Figure 13. $\dot{\phi}$ Relative Error

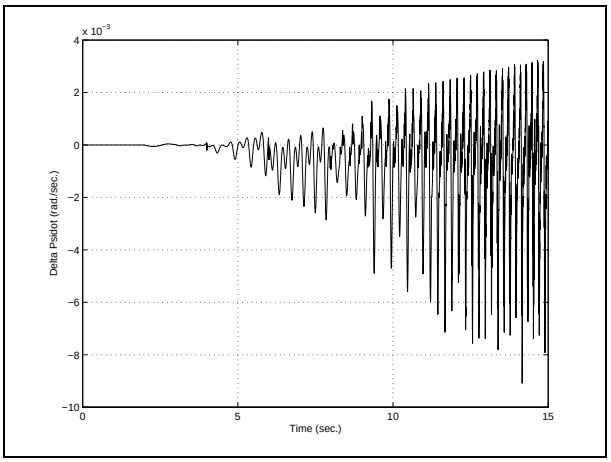

Figure 14. $\dot{\psi}$ Relative Error

CONCLUSIONS

The conclusions are as follows:

- The information contained in the Lagrangian of the two-gimbal gyroscope can be used directly to obtain a bond-graph formulation of the system.
- The two-gimbal gyroscope bond-graph obtained in this paper provides a more compact construction than the bond-graph given by Tiernego and van Dixhoorn [2]. The advantage that the Tiernego/van Dixhoorn representation has is one of symmetry in that the Eulerian Junction Structure (EJS) appears explicitly.
- A reduction in the state space of the gyroscope is possible by setting the effort source SE_6, and the initial condition of P_3, to zero. This reduction of order comes by direct inspection of the bond graph, yet is not readily apparent from the Lagrange equations.
- The simulation results for the Lagrange method and for the bond-graph are identical, baring small numerical differences. This result is fully expected since the bond-graph was obtained directly from the Lagrange equations.

REFERENCES

[1] L. Meirovitch. "Methods of ANALYTICAL DYNAMICS." McGraw-Hill, New York, NY, 1970.

[2] M. J. L. Tiernego, J. J. van Dixhoorn, "Three-axis platform simulation: Bond graph and Lagrangian Approach." *Journal of Franklin Institute*, vol. 308, n° 3, 1979, pp. 185-204.

[3] F. E. Cellier, "Continuous System Modeling." Springer Verlag, New York, USA, 1991.

[4] DYMOLA-dynamic modeling laboratory. World Wide Web page http://www.Dynasim.se, 1995.